



**HAL**  
open science

## Recent developments at the COMET instrument of the SEXTANTS beamline at SOLEIL

Horia Popescu, Kewin Desjardins, Victor Pinty, Alexandre Carcy, Cyril  
Leveille, Roland Gaudemer, Maurizio Sacchi, Nicolas Jaouen

► **To cite this version:**

Horia Popescu, Kewin Desjardins, Victor Pinty, Alexandre Carcy, Cyril Leveille, et al.. Recent developments at the COMET instrument of the SEXTANTS beamline at SOLEIL. *Journal of Physics: Conference Series*, 2022, 2380 (1), pp.012046. 10.1088/1742-6596/2380/1/012046 . hal-03940362

**HAL Id: hal-03940362**

**<https://cnrs.hal.science/hal-03940362v1>**

Submitted on 16 Jan 2023

**HAL** is a multi-disciplinary open access archive for the deposit and dissemination of scientific research documents, whether they are published or not. The documents may come from teaching and research institutions in France or abroad, or from public or private research centers.

L'archive ouverte pluridisciplinaire **HAL**, est destinée au dépôt et à la diffusion de documents scientifiques de niveau recherche, publiés ou non, émanant des établissements d'enseignement et de recherche français ou étrangers, des laboratoires publics ou privés.



Distributed under a Creative Commons Attribution 4.0 International License

PAPER • OPEN ACCESS

## Recent developments at the COMET instrument of the SEXTANTS beamline at SOLEIL

To cite this article: Horia Popescu *et al* 2022 *J. Phys.: Conf. Ser.* **2380** 012046

View the [article online](#) for updates and enhancements.

You may also like

- [K-shell photoionization of Be-like and Li-like ions of atomic nitrogen: experiment and theory](#)

M M Al Shorman, M F Gharaibeh, J M Bizau *et al.*

- [Education and training in radioecology during the EU-COMET project—successes and suggestions for the future](#)

Clare Bradshaw, Lindis Skipperud, Nicholas A Beresford *et al.*

- [K-shell photoionization of B-like oxygen \( \$O^{3+}\$ \) ions: experiment and theory](#)

B M McLaughlin, J M Bizau, D Cubaynes *et al.*

### ECS Toyota Young Investigator Fellowship



For young professionals and scholars pursuing research in batteries, fuel cells and hydrogen, and future sustainable technologies.

At least one \$50,000 fellowship is available annually.  
More than \$1.4 million awarded since 2015!



Application deadline: January 31, 2023

**Learn more. Apply today!**

# Recent developments at the COMET instrument of the SEXTANTS beamline at SOLEIL

Horia Popescu<sup>1</sup>, Kewin Desjardins<sup>1</sup>, Victor Pinty<sup>1</sup>, Alexandre Carcy<sup>1</sup>, Cyril Leveille<sup>1</sup>, Roland Gaudemer<sup>1</sup>, Maurizio Sacchi<sup>1,2</sup>, and Nicolas Jaouen<sup>1</sup>

<sup>1</sup>Synchrotron SOLEIL, L'Orme des Merisiers, 91192 Gif-sur-Yvette, France

<sup>2</sup>Institut des NanoSciences de Paris, CNRS, Sorbonne Université, 75005 Paris, France

horia.popescu@synchrotron-soleil.fr

**Abstract.** The COMET experimental station at SEXTANTS beamline of the SOLEIL synchrotron is dedicated to the coherent imaging of magnetic domains, using holography and ptychography, in a sample environment including magnetic fields up to 0.9 T, temperature range from 30 to 400 K and RF pumping. The 2D-detector capabilities of COMET were recently upgraded by adding to the standard CCD camera two new detectors: a high repetition rate 2D CMOS and a double delay line MCP for time resolved experiments. The three detectors can be interchanged within minutes without breaking the vacuum. The distance between an individual detector and the sample can be varied over a wide range, allowing for a trade-off between pixel size and field of view in the image reconstruction. A reconstructed pixel size of the order of 10 nm has been achieved with the new COMET setup. We report also a comparison between holographic images of magnetic domains obtained for the same sample by using the CMOS and the CCD detectors

## 1. Introduction

Resonant scattering of polarized soft x-rays is a field that encompasses several techniques, notably inelastic scattering, Raman spectroscopy, reflectivity, diffraction and coherent scattering; the SEXTANTS beamline [1] of the SOLEIL synchrotron is among the beamlines that comprehensively implement the ensemble of these techniques. The COMET [2] experimental station (**CO**herent **M**agnetic scattering **E**xperiments in **T**ransmission) is a high vacuum set-up placed at the intermediate focal point of the elastic branch of the SEXTANTS beamline. The instrument, which was opened to external users in 2015, is optimized for studying magnetic materials using holography [3] and ptychography, i.e. imaging techniques based on the coherent scattering of soft x-rays in transmission with variable angle of incidence. Several successful experiments were performed at COMET making use of the available sample environments, which comprise for instance magnetic fields up to 0.9 T, 30-400 K temperature range and radio-frequency pumping pump [4-8]. In all these experiments, the scattering diagrams were recorded using a 2D charge-coupled device (CCD) detector (Princeton Instruments), providing images with an optimal reconstructed pixel size of ~20 nm.

In this paper we report on the upgrade of the COMET end-station, with the addition of two new detectors: a 2D CMOS with higher repetition rate and a 2D time-resolved delay-line micro-channel plate (MCP-DL) detector opening up new opportunities for time resolved experiments. All the detectors can



now approach the sample at closer distance, allowing to collect the scattered intensity over wider angles and ultimately providing better spatial resolution in the reconstructed images.

## 2. COMET instrument design:

### 2.1. Vacuum chambers:

The COMET instrument is composed of two main vessels placed on the same marble table (fig 1), one for the sample environment (left) and the other dedicated to the three 2D detectors (right). The access to the sample environment is ensured by a quick-access lateral door. Differential pumping segments placed before and after the COMET vessels allow a fast beam return after a sample change, typically within 45 minutes.

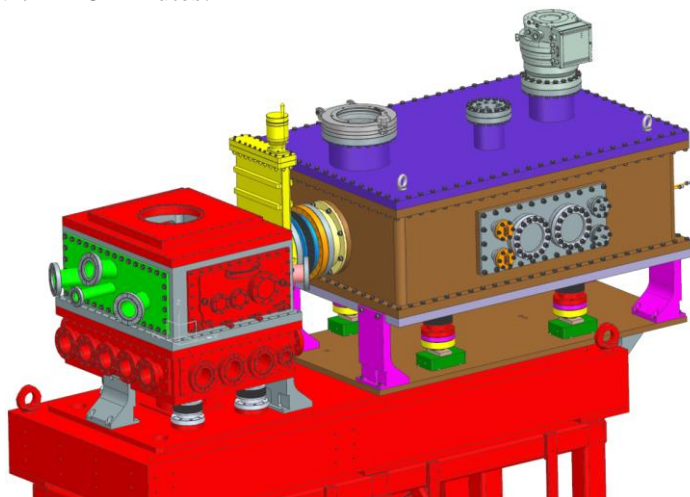


**Figure 1.** Engineer design of the new vacuum chamber. The left cube is the sample chamber. The right rectangular vessel hosts the three 2D detectors.

### 2.2. Sample environment

The sample holder is fixed on a robust MiCos XYZ-theta encoded stepper motors block (fig 2). The three translations have 35 mm travel and the rotation can turn the incidence angle of the beam on the sample between  $-45^\circ$  to  $+30^\circ$ . A flexible copper strip ensures the thermal contact with the He cryo-cooler. Both the cooler and the sample holder have integrated resistive heaters for precise temperature regulation, between 30 and 400 K with 0.1 K stability.

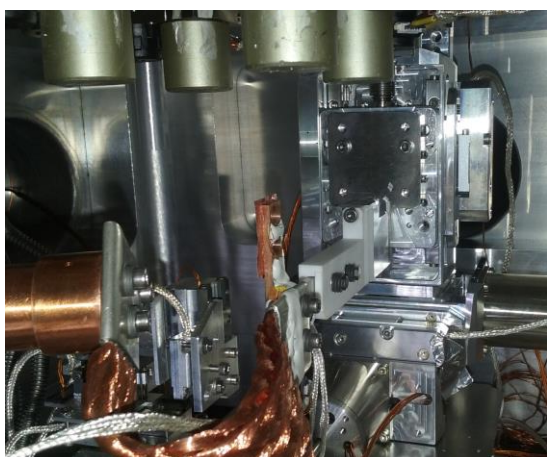


**Figure 2.** Internal mechanics with the XYZ-theta sample holder, connected to the He cryo-cooler, and the electrical contacts. The top part of the picture shows the cylindrical permanent magnets in retracted position.

A block of four cylindrical NdFeB permanent magnets can be inserted from the top in order to apply a controllable magnetic field on the sample. The field strength can be tuned by changing the height and the gap between the magnets. Each magnet can turn around its own axis and the combination of the height, gap and individual rotations makes it possible to set the resulting static field at the sample

position to a precise horizontal direction and custom magnitude up to 0.9 T. A Hall sensor integrated in the sample holder provides continuous monitoring of the applied field.

### 2.3. New 2D detectors

The detector part was recently upgraded with the addition of two new detectors (fig 3). The switching between the different detectors can be done within 15 minutes using an *in vacuo* 2 axes motorized encoded carriage. The sample to detectors distance can be tuned from 16 to 68 cm along the beam propagation direction.

The original CCD detector is maintained in service. Compared to the previous version, the new setup makes it possible to bring the CCD sensor closer to the sample (16 cm) and thus to increase the maximum collected angle in the scattering diagram on the 27 x 27 mm<sup>2</sup> chip. Consequently, the reconstructed pixel size is now half the previous values, reaching for instance ~10 nm at the photon energy of 778 eV (Co L<sub>3</sub>-edge).



**Figure 3.** Pictures of the internal mechanics showing the old CCD (front) and the new CMOS (back) detectors installed on their internal carriages, and of the MCP-DL detector. Each detector can be positioned on the x-ray beam axis and the displaced along it with a travel of 52 cm, in order to adjust the sample-detector distance.

The new 2D Complementary Metal Oxide Semiconductor (CMOS) detectors rival the performance of state-of-the-art photon detectors for optical applications. In the hybrid gain mode (suitable for high dynamic range) this detector runs at 24 frames/second in full chip, outperforming the classic CCD detectors that have a typical 4 seconds readout time and are limited to ~0.2 frames/second in full chip mode. In our experiments, the typical CCD exposure time per frame is of a few tenths of a second, i.e. an order of magnitude smaller than the CCD readout time, leading to a very inefficient duty cycle where most of the beamtime is spent for the readout. The new CMOS detector overcomes this limitation efficiently. The only drawback concerns the slightly smaller size of the chip (22.5 mm, corresponding to 2048 pixels 11  $\mu\text{m}$  in size), limiting the reconstructed pixel size for a given sample-detector distance. Together with a bulkier case that limits the sample-chipset minimum distance, the smallest pixel size of a reconstructed image at the Co-L<sub>3</sub> edge is 13 nm with the CMOS detector.

The CMOS prototype for in-vacuum soft x-ray applications was developed by the Soleil detector group and tested on several beamlines at Soleil [9] and, as a single shot detector, at the FERMI FEL source [10]. It is now available as a commercial product at Axis Photonique [11].



The third 2D detector, developed by the detector group from ELETTRA – Sincrotrone Trieste [12], is based on a micro-channel plate coupled to two transverse delay lines (MCP-DL). The time encoding technique of the spatial information (the conversion of the propagation time through the delay line into a spatial coordinate) works as a “single count” detection system within one start-stop temporal window, this being an essential requirement in time-resolved acquisitions. The detector can work up to 50 Mcounts/s. In high throughput experiments the incident photon flux must be attenuated in order to measure less than one photon within one temporal window. This makes a 2D time resolved detector with 60  $\mu\text{m}$  spatial resolution and 27 ps temporal resolution, capable of distinguishing the signal generated by every individual pulse of the synchrotron beam. The detector, intended for applications in time-resolved studies, notably stroboscopic pump-probe measurements, was already tested at the Tempo beamline of Soleil by measuring the fast demagnetization of a CoPd sample [13]. It will become particularly useful with the implementation of an infra-red laser (780 nm wavelength, from Spectra Physics), which is underway at the SEXTANTS beamline. This new laser system, expected to be operational by the end of 2022, will be synchronized with the synchrotron RF and will deliver 100 fs long pulses at 1 KHz repetition rate, with up to 7 mJ per pulse.

The new detection system comprises a central beam-stop that can be used to block the intense transmitted beam and gain in sensitivity for measuring the weak high-angle scattering signal. The beam-stop is no longer attached to a single detector but is now located in the sample chamber and will serve for all the three detectors. Two beam-stop sizes are available, one of 3 mm diameter for SAXS experiments, and one of 300  $\mu\text{m}$  diameter for holography and ptychography. The frame is mounted on an XYZ encoded piezo SmarAct block, with 31 mm travel in each direction. The supplementary axis along the beam propagation direction ensures a fine tuning of the beam-stop shadow on the detector and can be useful in some situations for facilitating the process of the image reconstruction.

### 3. Holography comparison between CCD and CMOS:

We used a test sample for comparing holographic reconstructed images using the CMOS and the CCD detectors (fig 4). For both acquisitions, the sample was maintained in the same magnetic state and the total exposure time was 500 sec.

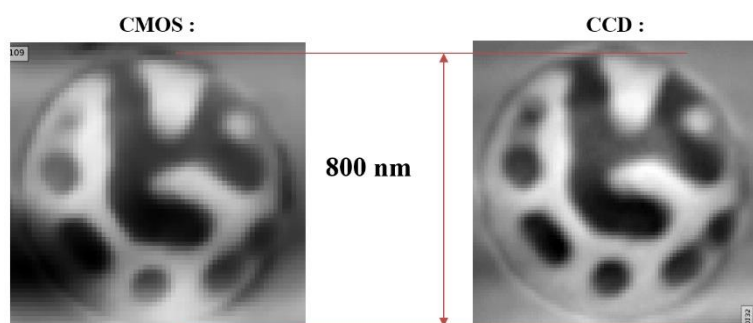


**Figure 4.** Reconstructed holographic images of the same sample obtained from data collected using either the CMOS (left) or the CCD (right) detector. The total exposure time is 500 s for both images.

For the CCD, the 500 seconds exposure time corresponded to 500 frames at 1 frame/second, which makes a total acquisition time of 50 minutes when including the readout. The CMOS recorded 1000 frames at 2 frame/second, for a total acquisition time of 8 minutes, with an evident gain in efficiency for producing an image with the same total exposure time. The CCD image quality is slightly better than the CMOS because of the smaller reconstructed pixel size (CMOS chip size is 22.5 mm, compared to the CCD chip size of 27 mm). While the quantum efficiency (QE) is almost the same at these energies for both detectors (0.85 for the CCD and 0.8 for the CMOS), the final contrast can get higher with the CCD due to the lower dark noise (0.02  $e^-/s/pixel$  for the CCD, versus 3  $e^-/s/pixel$  for the CMOS). The higher CCD readout noise (10  $e^-$  for the CCD versus 2  $e^-$  for the CMOS) is partly compensated by the number of acquired frames being usually higher for the CMOS. The image post processing, mainly for the beam-stop treatment, generates some reconstruction artefacts (shadows, border effects) that are also

different because of the difference in the beam-stop shadowing over the two sensors. For the same total exposure time the quality of the CCD is generally better, but overall the two images are comparable and the CMOS quality can easily be increased with higher statistics thanks to the much faster readout.

As an additional advantage, it should be mentioned that, in the relatively frequent case of damage by x-ray over-exposure, the chip replacement is faster and less expensive for the CMOS detector compared to the CCD one.

#### 4. Conclusion

The COMET instrument at the SEXTANTS beamline of the SOLEIL synchrotron has been recently upgraded with the integration of two new detectors, in addition to the CCD one. These new detectors are a fast 2D CMOS (24 frames/sec) and a 2D time-resolved delay line MCP-DL. The internal mechanics allows to position them closer to the sample, achieving an improved spatial resolution in the reconstructed images. The new design offers also a fast access to the detectors' vessel, facilitating interventions and operations on the detectors themselves.

In the course of the year, the combination of the time-resolved detector with the installation of the ultra-fast IR laser source under construction will open new possibilities for pump-probe experiments at COMET.

#### Acknowledgements

We thank Riccardo Battistelli, Matthieu Grelier, Felix Buettner, Nicolas Reyren and Vincent Cros for the test sample and the image reconstruction using phase retrieval holography.

#### References

- [1] Sacchi M. *et al.* 2013 The SEXTANTS beamline at SOLEIL: a new facility for elastic, inelastic and coherent scattering of soft X-rays *J. Phys.: Conf. Series* **425** 072018
- [2] Popescu H. *et al.* 2019 COMET: a new end-station at SOLEIL for coherent magnetic scattering in transmission *J. Synch. Rad.* **26** 280-290
- [3] Eisebitt S. *et al.* 2004 Lensless imaging of magnetic nanostructures by X-ray spectro-holography *Nature* **432** 885-888
- [4] Bukin N. *et al.* 2016 Time-resolved imaging of magnetic vortex dynamics using holography with extended reference autocorrelation by linear differential operator *Sci. Rep.* **6** 36307
- [5] Le P. T. P. *et al.* 2020 Tailoring Vanadium Dioxide Film Orientation Using Nanosheets: a Combined Microscopy, Diffraction, Transport and Soft X-Ray in Transmission Study *Adv. Func. Mater.* **30** 1900028
- [6] Loudon J. C. *et al.* 2019 Do Images of Biskyrmions Show Type-II Bubbles? *Adv. Mater.* **31** 1806598
- [7] Birch M. T. *et al.* 2020 Real-space imaging of confined magnetic skyrmion tubes *Nature Commun.* **11** 1726.
- [8] Turnbull L. A. *et al.* 2021 Tilted X-Ray Holography of Magnetic Bubbles in MnNiGa Lamellae. *ACS Nano* **15** 387-395
- [9] Desjardins K. *et al.* 2020 Backside-illuminated scientific CMOS detector for soft X-ray resonant scattering and ptychography *J. Synch. Rad.* **27** 1577-1589
- [10] Leveille C. *et al.* 2022 Single-shot experiments at the soft X-FEL FERMI using a back-side-illuminated scientific CMOS detector *J. Synch. Rad.* **29** 103-110
- [11] <https://www.axis-photon.com/streak-camera/axis-sxr-soft-x-ray-scmos-camera/>
- [12] Cautero G. *et al.* 2008 *Nucl. Instrum. Methods Phys. Res. A* **595** 447-459
- [13] Silly M. G. *et al.* 2017 Pump-probe experiments at the TEMPO beamline using the low- $\alpha$  operation mode of Synchrotron SOLEIL *J. Synch. Rad.* **24** 886-897